Irradiation-induced M1 Microglia Affect Brain Metastatic Colonization of A549 Cell Lines via miR-9/CDH1 Axis

Yu Jin
Tongji Hospital of Tongji Medical College of Huazhong University of Science and Technology
https://orcid.org/0000-0002-3427-4937
Yalin Kang
Tongji Hospital of Tongji Medical College of Huazhong University of Science and Technology
Wan Qin
Tongji Hospital of Tongji Medical College of Huazhong University of Science and Technology
Qianxia Li
Tongji Hospital of Tongji Medical College of Huazhong University of Science and Technology
Qi Mei
Tongji Hospital of Tongji Medical College of Huazhong University of Science and Technology
Xinyi Chen
Tongji Hospital of Tongji Medical College of Huazhong University of Science and Technology
Guangyuan Hu
Tongji Hospital of Tongji Medical College of Huazhong University of Science and Technology
Yang Tang
Tongji Hospital of Tongji Medical College of Huazhong University of Science and Technology
Xianglin Yuan (yuanxianglin@hust.edu.cn)
Tongji Hospital of Tongji Medical College of Huazhong University of Science and Technology
https://orcid.org/0000-0003-4653-5388

Research

Keywords: brain metastasis, non-small-cell lung cancer, cranial irradiation, E-cadherin protein, M1-microglia polarization, miR-9

Posted Date: December 11th, 2020

DOI: https://doi.org/10.21203/rs.3.rs-123435/v1

Abstract

Background and purpose: Brain metastasis is among the leading causes of death in patients with non-small-cell lung cancer (NSCLC). Through yet unknown mechanisms, prophylactic cranial irradiation (PCI) can significantly decrease the incidence of brain metastases. We propose that PCI probably exerts indirect anti-tumoral effects by turning cerebral “soil” unfavorable for the colonization of metastatic tumor “seeds”. This study aims to reveal how PCI regulates the brain microenvironment conducing to a reduction in brain metastases.

Materials and methods: Key marks of M1/M2 microglia types and mesenchymal-to-epithelial transition (MET) were analyzed by qRT-PCR and Western Blot in vitro. The target miR-9-5p was obtained by miRNA array analysis and confirmed by qRT-PCR in microglia. miRTarBase and TargetScan were used to predict the target genes of miR-9-5p, which were assessed by luciferase activity assay. Anti-metastatic effects of irradiation on the brain were evaluated by intravital imaging using a brain metastatic NSCLC A549-f3 cell line in a nude mouse model.

Results: We found the microglia can polarize into M1 type after irradiation and the irradiated microglia inhibited mesenchymal-epithelial transition of metastatic tumor cells, which decreased their adhesion and colonization capabilities in brain. We discovered up-regulated miR-9 was related with inhibition of MET process. Further overexpression/silencing experiments indicated that irradiated M1-type microglia inhibited A549 mesenchymal-epithelial transition, mediated by miR-9 up-regulation and secretion. Additionally, these results were confirmed in mice model, as low dose irradiation increased miR-9 level in the brain microenvironment and reduced brain metastases of metastatic tumor cells.

Conclusions: We demonstrated that miR-9 secreted by irradiated M1-type microglia played important role in inducing A549 cell lines into mesenchymal phenotype, and further decreased their localization capabilities in brain. Our findings emphasized the modulating effect of irradiation on metastatic soil, and the cross-talk between tumor cells and the metastatic microenvironment. More importantly, our findings provided new perspectives for effective anti-metastasis therapies, especially for NSCLC patients with high risk of brain metastasis.

Background

Lung cancer is among leading causes of premature mortality worldwide, accounting for over 142,670 cancer-related deaths in the United States in 2019[1, 2]. Metastasis is the main cause of death in lung cancer patients; with brain metastasis (BM) being common among both small-cell lung cancer (SCLC) and non-small cell lung cancer (NSCLC) patients[3]. Despite recent progress in diagnosis and treatment of BM, the associated overall median survival estimates remain at < 6 month[4]. Prophylactic cranial irradiation (PCI) was introduced in 1980 as a method to prevent brain metastasis[5]. Randomized clinical trials and a meta-analysis have shown that PCI was concerned with improved survival in patients with SCLC[6, 7]. As for NSCLC patients, the RTOG 0214 trial demonstrated that the incidence of BM was lower

in the PCI (7.7%) than in the non-PCI group (18%) but there is no overall survival benefit[8]. Thus, there is an urgent need to uncover the molecular mechanism of PCI in reducing brain metastasis and find alternative therapies.

On the one hand, the irradiation dosage used in PCI (usually < 25 Gy in total) is insufficient to have tumoricidal effects. On the other, accounting for the persistent protective effect months after PCI treatment remains challenging. Some authors have suggested that irradiation has a modulating effect on the brain local immune system[9, 10]. In fact, studies have demonstrated that a microenvironmental change in a distant organ can influence the rate of colonization of metastatic tumor cells[11, 12]. Based on these results, our group proposed that PCI might alter the “soil” in the brain protecting it against the colonization of a tumor “seed”. Microglia, a resident macrophage, is a major constituent of the brain immune system, playing a vital role in the cerebral microenvironment[12]. Presence of different microglia phenotypes, including M1 and M2, has been previously suspected[13, 14]. Moreover, it has been proposed that under LPS stimulation, microglia turn into M1 type and exhibit a pro-inflammatory phenotype, which leads to tumor growth inhibition[12, 15, 16]. However, activation of IL4 and IL10, microglia produce an M2 phenotype. M2 microglia produce anti-inflammatory and immune response-suppressive factors and create a microenvironment favorable to tumor proliferation[12, 15, 17].

Studies on metastases have demonstrated that lung cancer cells affect several vital pathways, including those associated with evading immune system surveillance[18] and developing chemotherapy resistance[19], both of which can facilitate metastatic behavior and disease progression. Notably, during the metastatic process, tumor cells undergo a morphological change that involves regulating multiple adhesion and cellular matrix molecules to acquire a mesenchymal phenotype. This phenomenon, called epithelial-to-mesenchymal transition (EMT), dramatically increases the rates of extravasation, blood/lymphatic vessel invasion, and distant organ reach of tumor cells[20, 21]. When metastatic tumor cells travel to a distant organ, the reverse process occurs, mesenchymal-to-epithelial transition (MET), enabling these cells to up-regulate expression of various adhesion molecules, localizing then in proximity and forming metastatic loci[22]. Meanwhile, studies indicate that microRNA plays an important role in the regulation of the EMT/MET process[23]. To explore the detailed MET inhibitory mechanism of irradiated M1 microglia on A549 cells, we performed a meta-study on microRNA expression by profiling a murine microglia cell model.

Therefore, we hypothesized that irradiated microglia might alter the phenotypical transition process of tumor cells and distant organ localization, which in turn lower the chances of brain metastasis. Here, we aimed to discover the polarization effect of irradiation on microglia, and to further explore the underlying mechanism of the inhibitory effects of microglia on tumor cell MET transition after ionized irradiation treatment.

Materials And Methods

Cell lines and irradiation treatment

Human microglia cell lines CHME-5 and HMO6, human glioma cell line U87, human lung cancer cell line A549 and human renal epithelial 293T cells were purchased from Cellbank, Chinese Academy of Sciences, China. A549-F3 are brain metastatic cells derived from parental A549 cells through three rounds of in vivo selections with mice model. Cells were cultured in DMEM and RPMI 1640 medium (HyClone, Logan, UT), supplemented with 10% FBS (Gibco, Grand Island, NY), and cultured in a humidified incubator with 5% CO2 at 37 °C. The mesenchymal phenotype of A549 cells was induced with recombinant human TGF-β1 (PeproTech;100-21C). Cells were irradiated using a RS2000 X-ray Biological Research Irradiator (25 mA, 160 kV; Rad Source Technologies Inc., Suwanee, GA).

Western blot analysis

Western blot was conducted as described previously[24]. Primary antibodies of iNOS (1:400; Boster, BM4828), Arg1 (1:1000; Cell Signaling Technology, #93668), E-Cadherin (1:100; Abcam; ab1416), Vimentin (1:1000; Abcam; ab8978), GAPDH (1:8000; Boster, BM1985), α-Tublin Ab (1:2000, 11224-1-AP; Proteintech) were used. The membranes were tested with an ECL detection system (Thermo Fisher Scientific, Waltham, MA).

Immunofluorescence

Briefly, CHME5 cells were seeded on glass slides and fixed with 4% paraformaldehyde. After cell attachment, slides were incubated with a primary antibody specific to iNOS (1:50, 18985-1-AP; Proteintech) overnight at 4 °C, followed by Cy3-conjugated secondary antibody for 1 hour. Later, cell nuclei were stained with DAPI for 5 minutes (Promoter, Wuhan, China). Immunofluorescence was captured under fluorescence microscope (DMI3000B; Leica Microsystems, Shanghai, China) and qualitatively analyzed by ImageJ software.

Quantitative Real-time PCR

Quantitative RT-PCR was conducted as described previously[24]. The primers used for GAPDH, IL-10, IL1B, iNOS are listed in Supplementary Table 1. To analyze miRNA expression, we used miDETECT A Track miRNA qRT-PCR Kit and a Bulge-Loop miRNA qRT-PCR Kit (RiboBio, Guangzhou, China) for reverse-transcribed, according to the manufacturer's introduction. Expression levels were normalized to those of U6-snRNA expression. All experiments were performed in triplicate.

MicroRNA array analysis

Microarray data were retrieved from Freilich[15] and Gene Expression Omnibus (GEO, http://www.ncbi.nlm.nih.gov/geo, accession number GSE49330). Analytical pipeline was established according to the description by Yang et al [25]. Raw gene-chip data (gene chip type Mouse GeneChip miRNA 2.0 Array) were downloaded and analyzed with J-Express software package (Version 2012, Department of Informatics, University of Bergen, Norway). Chip data were calculated with the robust multichip analysis (RMA) to form datasets of log2-transformed probe set values. Genes significantly different in expression level were identified by the SAM method (FDR < 1%), and data with group fold

change > 4 or ≤4 were extracted and analyzed with unsupervised hierarchical clustering (Pearson correlation).

Plasmid transduction

We purchased negative control oligonucleotides, mimics and inhibitors of miR-9 from GeneChem (Shanghai, China). A549 cells and A549-F3 cells were transfected with oligonucleotides using Lipofectamine 2000 reagent (11668-019, Invitrogen), according to the manufacturer's instructions.

Luciferase activity assay

We found E-cadherin (also known as CDH1) was a potential target of miR-9 using TargetScan and miRTarBase software. Luciferase reporter assays were performed as described in the manufacturer's protocol. In short, the pMIR-REPORT-CDH1-3'UTR(WT) or pMIR-REPORT-CDH1-3'UTR(MUT) and miR-9-5p or scramble miRNA mimic were transfected into 293T cells. After co-transfection for 48 h, luciferase activities were measured by Dual-Luciferase Reporter Assay System (E1910, Promega), using fluorescence microscope (MHG-100B, MOTIC).

Animal studies

All animal work was done in accordance with the National Institutes of Health guide for the care and use of Laboratory animals. For brain metastasis experiments, male BALB/c nude mice (6-to-8-week-old) were raised in pathogen-free conditions. The mice were randomly divided into two groups. In the irradiated group, mice were treated with 3 Gy*2f of irradiation to the whole brain and raised for 1 week. Subsequently, 100 μl PBS containing 2×10^5 luciferase-labeled A549-F3 cells was injected into the left cardiac ventricle of each mouse. At the end of the experiment, mice were sacrificed and examined for brain metastases.

Intravital imaging and analysis

Mice received an intra-peritoneal injection of 150 ul of 1.5% D-luciferin and anaesthetized with 1.5% chloral hydrate. Imaging was completed with a Xenogen IVIS system (Caliper) coupled to Living Image Acquisition and Analysis software (Xenogen). For BLI plots, photon flux was calculated for each mouse by using a rectangular region of interest encompassing the mouse's thorax.

Statistical analyses

Statistical calculations were performed using GraphPad Prism 8.0.1 (GraphPad Software, CA, USA). Statistical comparisons between experimental groups were performed with a two-tailed Student t-test. Data are shown as mean ± SD. $P < 0.05$ was considered indicative of significant findings.

Results

Irradiated microglia exhibited M1-type polarization and hampered A549 cells MET transition

To explore the impact of irradiation on microglial phenotype, CHME5 cells were treated with 0, 2, 3, 4 Gy of irradiation. Then the mRNA levels of iNOS and IL10 as the markers for M1 and M2 types, respectively, were measured. There was a noticeable up-regulation in iNOS expression and down-regulation of IL 10 expression in irradiated microglia, particularly in the group treated with 3 Gy (Fig. 1A). Western Blot analysis revealed up-regulation of iNOS expression and down-regulation of Arg1 expression after treatment with 3 Gy irradiation (Fig. 1B). Further analysis showed that the effects of irradiation were extremely obvious at 48 h using qRT-PCR and Western Blot (Fig. 1C and 1D). Immunofluorescence staining results were consistent with these observations (Fig. 1E).

Next, we plan to explore the role of irradiated M1 microglia on the phenotypical modulation of NSCLC cells. The expression of E-cadherin and Vimentin in A549 cells was analyzed by Western Blot, both of which vital markers of epithelial/mesenchymal phenotype. In the group with control culture media, the mesenchymal phenotype A549 cells quickly reversed into epithelial type with high E-cadherin and low Vimentin expression. In contrast, in the group treated with irradiated CHME5 supernatant, A549 cells retained their mesenchymal phenotype with low E-cadherin and high Vimentin expression. Introduction to these groups of CHME5 supernatant without irradiation or U87 supernatant did not affect the observed phenotype changes (Fig. 1F).

Irradiation-induced M1 microglia increased both intra and extra-cellular miR-9 level

Several recent studies indicated microRNAs played crucial roles in regulation of EMT/MET process[26, 27]. Thus, we analyzed microRNA expression in LPS-treated group and control groups. miR-9 levels increased dramatically in LPS-induced M1 microglia (Fig. 2A). We confirmed that the level of miR-9 was significantly elevated in irradiated CHME5 and HMO6 cells (3 Gy and 3 Gy*2f), when compared with non-irradiated microglia, both intracellularly (Fig. 2B and 2D) and extracellularly (Fig. 2C and 2E). These results showed that miR-9 expression was up-regulated in irradiated microglia and it was secreted into the extracellular space, suggesting that miR-9 secreted by irradiated microglia played an important role in inducing a mesenchymal phenotype in metastatic A549 cells.

Irradiated M1-type microglia elevated intracellular level of miR-9 in A549 cell lines

To confirm the effects of miR-9 produced by irradiated M1 microglia on the MET process, we modulated the expression of miR-9 in A549 or brain metastatic A549-F3 cells, using an miR-9 mimic and inhibition of plasmid transduction (Fig. 3A and 3B). Levels of intracellular miR-9 were detected via qRT-PCR in each of three groups: negative control, over-expression, and inhibition group. Significantly elevated/decreased miR-9 levels were detected in the overexpression/inhibition group respectively, confirming the success of in vitro miR-9 expression modulation in A549 and A549-F3 cells (Fig. 3C and 3D).

We added irradiated or non-irradiated microglia culturing supernatant into A549 and A549-F3 cells transfected with control/miR-9 mimic/miR-9 inhibition plasmid, respectively, observing the highest level of miR-9 in miR-9 mimic group treated with irradiated conditioned medium. In contrast, the lowest miR-9 level were detected in the miR-9 inhibition group, where the non-irradiated microglia supernatant was

added (Fig. 3E and 3F). When the miR-9 inhibition A549/A549-F3 group was treated with irradiated microglia supernatant, their intracellular levels of miR-9 were significantly higher than those in the miR-9 inhibition group treated with non-irradiated microglia supernatant. This result suggests that irradiated M1 microglia increased their production and secretion of miR-9; and so, the uptake of miR-9 by A549 and A549-F3 was increased. This absorbed miR-9 might play a role in reducing NSCLC brain metastasis.

Irradiated M1 type microglia inhibited the MET via miR-9/CDH1

To explore the influence of miR-9 levels on phenotypic conversions of A549 and A549-F3 cells we conducted Western blot analysis. In Fig. 4A, groups with controlled culture media and negative plasmid the mesenchymal phenotype A549 cells quickly reversed into epithelial-type with high E-cadherin and low Vimentin expression. In contrast, groups with up-regulated miR-9 retained their mesenchymal phenotype (low E-cadherin and high Vimentin expression). Among groups with up-regulated miR-9, those treated with irradiated microglia supernatant retained the most typical mesenchymal phenotype. Meanwhile, miR-9 downregulation could promote E-cadherin expression. Furthermore, A549 cells with down-regulated miR-9 treated with non-irradiated microglia supernatant transformed into the most typical epithelial phenotype (the highest E-cadherin and the lowest Vimentin expression). Consistent with the above, A549-F3 cells transfected with down-regulated miR-9 plasmid were able to develop an epithelial phenotype, while irradiated microglia supernatant could inhibit the MET process to keep the A549-F3 cells in a mesenchymal state. Meanwhile, A549-F3 cells with up-regulated miR-9 treated with irradiated CHME5 supernatant maintained the most typical mesenchymal phenotype (Fig. 4B).

Given that, miRNAs could inhibit gene expression by binding to the 3'UTR of respective RNAs [28], WT and MUT of CDH1 3'UTR-driven luciferase vectors were respectively cotransfected with NC or miR-9-5p mimics into 293T cells (Fig. 4C). Results indicated cotransfection with miR-9-5p mimics and WT CDH1 3'-UTR caused inhibition of luciferase activity. Moreover, cotransfection of miR-9-5p mimics and MUT CDH1 3'-UTR had no effects on luciferase activity Fig. 4D). These findings point to CDH1 being the target of miR-9.

Low dose irradiation reduced brain metastases of A549-F3 cells in brain mice model

To confirm the effects of irradiation on NSCLC-BM in vivo, we selected 7 days after irradiation to inject tumor cells for the higher level of miR-9 (Fig. S1). We use bioluminescence imaging (BLI) to assess the incidence rate of BM in a mouse model (Fig. 5A and 5B). BM incidence was reduced in irradiated mice (40%, n = 10), when compared to the control group (70%, n = 10) (Fig. 5C). There are significant differences between the two groups by analysis of the photon flux (Fig. 5D). Furthermore, irradiation increased miR-9 levels in mice brain microenvironment (Fig. 5E). These findings suggest that, in a mouse model, low dose irradiation reduces A549-F3 cells-mediated brain metastases, plausibly by elevating miR-9 expression levels, which inhibit tumor cells MET in brain microenvironment.

Discussion

In this study, we showed a significant shift towards M1 microglia phenotype after irradiation. Moreover, M1 microglia inhibited the MET process of A549 cell lines, a crucial step in their capacity for adhesion to and colonization of distant organs, in particular, the brain. MiRNA array analysis revealed up-regulated expression of miR-9 in M1 microglia. In addition, increased miR-9 secreted by irradiated M1 microglia played an important role in inhibition of the MET process. Finally, miR-9 exerted these effects by targeting CDH1, a gene vital to this process. Evidence from a mouse model supported the effects of irradiation-induced miR-9 elevation on lowering the incidence of brain metastasis in A549-F3 cells.

It has been well established that microglia localizing in brain parenchymal are main cellular constituent that are involved in brain innate immunity[29]. They detect “danger signals,” including presence of infectious agent, toxins and cell damage among others, using danger-associated-molecular-pattern receptors (DAMP) and trigger inflammatory responses[9, 13]. Here, our findings are consistent with previous studies that demonstrated that irradiation promoted M1 microglia activation and anti-metastatic effects[9, 10]. Concurrently, numerous studies have suggested that the pro-inflammatory status of M1 microglia showed anti-tumoral capacity via improved antigen presenting capabilities[30] and direct suppression of tumor growth[31]. This study revealed a novel mechanism of inhibitory effects on NSCLC cells localization, presumably by promoting miR-9 production and secretion from irradiated M1 microglia.

Recent studies have indicated that miR-9 exhibits anti-tumor effects by inhibiting tumor cell motility. Specifically, Ben-Hamo et al. demonstrated that overexpression of miR-9 in glioblastoma hampered tumor cell mobility, possibly via inhibition of the MAPK pathway, which subsequently disrupted cellular actin cytoskeleton organization[32]. In addition, Xu et al. showed that ectopic expression of miR-9 in melanoma cells suppressed the tumor capacity of migration and invasion. These authors identified the downstream target gene NRP1, negatively regulated by miR-9, as responsible for the change in motility of tumor cells[33]. Meanwhile, growing evidences have indicated that miR-9 plays a vital role in regulating the MET process and tumor cell metastasis[27, 34, 35]. In our research, through high-throughput micro-RNA profiling analysis, we observed significant miR-9 up-regulation in irradiated microglia. This increased miR-9 expression within A549 cell lines, in turn, promoted their mesenchymal phenotype. Eventually, decreased expression of adhesive molecules in metastatic tumor cells hampered their localizing capacity in the brain.

However, we must point out that our research has some limitations. For one hand, we only got preliminary results and have not verified the possibility of the target as an intervention treatment. For another, the present findings are based on cellular and animal models, while elucidating the molecular mechanism of irradiated effects on brain metastasis in NSCLC patients requires further studies involving human subjects.

Conclusions

In short, we found significant M1 polarization shifting of microglia after irradiation treatment. We demonstrated irradiation induced M1-type microglia significantly modulate metastatic A549 cell lines into

mesenchymal phenotype through up-regulating and secreting of miR-9, which eventually shifted tumor cell into mesenchymal phenotype and further decreased localization capabilities in brain. Our study firstly demonstrated that irradiated microglia modulated tumor cell MET process via miR-9/CDH1, providing new insights into PCI's mechanism. It might inform further studies on irradiation effects to tumor microenvironment. Clinically, miR-9 expression might act as predictive biomarker for brain metastasis in NSCLC patients. Moreover, treatments targeting the miR-9 pathway combined with radiotherapy might help reduce the risk of brain metastasis, providing novel perspectives for effective anti-metastatic therapies.

Abbreviations

SCLC, small cell lung cancer; NSCLC, non-small cell lung cancer; BM, brain metastasis; PCI, prophylactic cranial irradiation; IR, ionizing radiation; EMT, epithelial-to-mesenchymal transition; MET, mesenchymal-to-epithelial transition; DMEM, Dulbecco's minimal essential media; RMA, robust multichip analysis; LPS, Lipopolysaccharides; FBS, fetal bovine serum; PBS, Phosphate Buffered Saline; PCR, polymerase chain reaction; DAPI, diamidino-phenylindole; WT, wild type; MUT, mutant type; BLI, Bioluminescence imaging; UTR, untranslated regions; DAMP, danger-associated-molecular-pattern receptors; miRNAs, MicroRNAs; SD, standard deviation.

Declarations

Ethics approval and consent to participate

Not applicable.

Consent for publication

Not applicable.

Availability of data and materials

Not applicable.

Competing interests

The authors declare that they have no competing interests.

Authors' contributions

X.Y. and Y.T. directed and supervised the work. Y.J. performed the majority of laboratory experiments and drafted the manuscript. Y.K. performed the statistical analyses and revised the manuscript. W.Q. and X.C. performed additional laboratory experiments. Q.L., Q.M. and G.H. conceptualized and oversaw the project and revised the manuscript. All authors read and approved the final manuscript

Acknowledgements

This work received support from the National Natural Science Foundation of China (Grant no. 81773360) and the Engineering Research Center Innovation Capacity Building Project of Hubei (Grant no. 2018-420114-35-03-071705)

References

1. Bade BC, Dela Cruz CS: Lung Cancer 2020: Epidemiology, Etiology, and Prevention. *Clin Chest Med* 2020, 41(1):1-24.
2. Siegel RL, Miller KD, Jemal A: Cancer statistics, 2019. *CA Cancer J Clin* 2019, 69(1):7-34.
3. Yousefı M, Bahrami T, Salmaninejad A, Nosrati R, Ghaffari P, Ghaffari SH: Lung cancer-associated brain metastasis: Molecular mechanisms and therapeutic options. *Cellular Oncology* 2017, 40(5):419-441.
4. Li QX, Zhou X, Huang TT, Tang Y, Liu B, Peng P, Sun L, Wang YH, Yuan XL: The Thr300Ala variant of ATG16L1 is associated with decreased risk of brain metastasis in patients with non-small cell lung cancer. *Autophagy* 2017, 13(6):1053-1063.
5. Nakahara Y, Sasaki J, Fukui T, Otani S, Igawa S, Hayakawa K, Masuda N: The role of prophylactic cranial irradiation for patients with small-cell lung cancer. *Jpn J Clin Oncol* 2018, 48(1):26-30.
6. Bloom BC, Augustyn A, Sepesi B, Patel S, Shah SJ, Komaki RU, Schild SE, Chun SG: Prophylactic Cranial Irradiation Following Surgical Resection of Early-Stage Small-Cell Lung Cancer: A Review of the Literature. *Front Oncol* 2017, 7:228.
7. Aupérin A, Arriagada R, Pignon J-P, Le Péchoux C, Gregor A, Stephens RJ, Kristjansen PEG, Johnson BE, Ueoka H, Wagner H *et al*: Prophylactic Cranial Irradiation for Patients with Small-Cell Lung Cancer in Complete Remission. *New England Journal of Medicine* 1999, 341(7):476-484.
8. Sun A, Hu C, Wong SJ, Gore E, Videtic G, Dutta S, Suntharalingam M, Chen Y, Gaspar LE, Choy H: Prophylactic Cranial Irradiation vs Observation in Patients With Locally Advanced Non-Small Cell Lung Cancer: A Long-term Update of the NRG Oncology/RTOG 0214 Phase 3 Randomized Clinical Trial. *JAMA Oncol* 2019, 5(6):847-855.
9. Lumniczky K, Szatmari T, Safrany G: Ionizing Radiation-Induced Immune and Inflammatory Reactions in the Brain. *Front Immunol* 2017, 8:517.
10. Morganti JM, Jopson TD, Liu S, Gupta N, Rosi S: Cranial irradiation alters the brain's microenvironment and permits CCR2+ macrophage infiltration. *PLoS One* 2014, 9(4):e93650.
11. Zhang L, Zhang S, Yao J, Lowery FJ, Zhang Q, Huang WC, Li P, Li M, Wang X, Zhang C *et al*: Microenvironment-induced PTEN loss by exosomal microRNA primes brain metastasis outgrowth. *Nature* 2015, 527(7576):100-104.
12. Wu S-Y: The roles of microglia macrophages in tumor progression of brain cancer and metastatic disease. *Frontiers in Bioscience* 2017, 22(10):1805-1829.

13. Eggen BJL, Raj D, Hanisch UK, Boddeke HWGM: Microglial Phenotype and Adaptation. *Journal of Neuroimmune Pharmacology* 2013, 8(4):807-823.
14. Cheray M, Joseph B: Epigenetics Control Microglia Plasticity. *Frontiers in Cellular Neuroscience* 2018, 12.
15. Wei J, Gabrusiewicz K, Heimberger A: The controversial role of microglia in malignant gliomas. *Clin Dev Immunol* 2013, 2013:285246.
16. Yu H, Pardoll D, Jove R: STATs in cancer inflammation and immunity: a leading role for STAT3. *Nat Rev Cancer* 2009, 9(11):798-809.
17. Annovazzi L, Mellai M, Bovio E, Mazzetti S, Pollo B, Schiffer D: Microglia immunophenotyping in gliomas. *Oncol Lett* 2018, 15(1):998-1006.
18. Califano R, Kerr K, Morgan RD, Lo Russo G, Garassino M, Morgillo F, Rossi A: Immune Checkpoint Blockade: A New Era for Non-Small Cell Lung Cancer. *Current Oncology Reports* 2016, 18(9):59.
19. Acharyya S, Oskarsson T, Vanharanta S, Malladi S, Kim J, Morris PG, Manova-Todorova K, Leversha M, Hogg N, Seshan VE *et al*: A CXCL1 paracrine network links cancer chemoresistance and metastasis. *Cell* 2012, 150(1):165-178.
20. Davis FM, Stewart TA, Thompson EW, Monteith GR: Targeting EMT in cancer: opportunities for pharmacological intervention. *Trends Pharmacol Sci* 2014, 35(9):479-488.
21. Mirzaei H, Masoudifar A, Sahebkar A, Zare N, Sadri Nahand J, Rashidi B, Mehrabian E, Mohammadi M, Mirzaei HR, Jaafari MR: MicroRNA: A novel target of curcumin in cancer therapy. *J Cell Physiol* 2018, 233(4):3004-3015.
22. Gunasinghe NPAD, Wells A, Thompson EW, Hugo HJ: Mesenchymal–epithelial transition (MET) as a mechanism for metastatic colonisation in breast cancer. *Cancer and Metastasis Reviews* 2012, 31(3-4):469-478.
23. Legras A, Pécuchet N, Imbeaud S, Pallier K, Didelot A, Roussel H, Gibault L, Fabre E, Le Pimpec-Barthes F, Laurent-Puig P *et al*: Epithelial-to-Mesenchymal Transition and MicroRNAs in Lung Cancer. *Cancers* 2017, 9(12).
24. Yi M, Liu B, Tang Y, Li F, Qin W, Yuan X: Irradiated Human Umbilical Vein Endothelial Cells Undergo Endothelial-Mesenchymal Transition via the Snail/miR-199a-5p Axis to Promote the Differentiation of Fibroblasts into Myofibroblasts. *BioMed Research International* 2018, 2018:1-10.
25. Li Yang NYL, Li Zhu, Min Xiao DNMT3A R882 mutation is associated with elevated expression of MAFB and M4-M5 immunophenotype of acute myeloid. *Leukemia & Lymphoma* 2015, 56(10):9.
26. Park YR, Lee ST, Kim SL, Zhu SM, Lee MR, Kim SH, Kim IH, Lee SO, Seo SY, Kim SW: Down-regulation of miR-9 promotes epithelial mesenchymal transition via regulating anoctamin-1 (ANO1) in CRC cells. *Cancer Genet* 2019, 231-232:22-31.
27. Zhou B, Xu H, Xia M, Sun C, Li N, Guo E, Guo L, Shan W, Lu H, Wu Y *et al*: Overexpressed miR-9 promotes tumor metastasis via targeting E-cadherin in serous ovarian cancer. *Frontiers of Medicine* 2017, 11(2):214-222.

28. Bartel DP: MicroRNAs: genomics, biogenesis, mechanism, and function. *Cell* 2004, 116(2):281-297.
29. Wei J, Chen P, Gupta P, Ott M, Zamler D, Kassab C, Bhat KP, Curran MA, de Groot JF, Heimberger AB: Immune biology of glioma-associated macrophages and microglia: functional and therapeutic implications. *Neuro Oncol* 2020, 22(2):180-194.
30. Lahmar Q, Keirsse J, Laoui D, Movahedi K, Van Overmeire E, Van Ginderachter JA: Tissue-resident versus monocyte-derived macrophages in the tumor microenvironment. *Biochim Biophys Acta* 2016, 1865(1):23-34.
31. Sarkar S, Döring A, Zemp FJ, Silva C, Lun X, Wang X, Kelly J, Hader W, Hamilton M, Mercier P *et al*: Therapeutic activation of macrophages and microglia to suppress brain tumor-initiating cells. *Nature Neuroscience* 2013, 17(1):46-55.
32. Rotem Ben-Hamo AZ, Helit Cohen1 and Sol Efroni: hsa-miR-9 controls the mobility behavior of Glioblastoma cells via regulation of MAPK14 signaling elements. *OncoTargets and Therapy* 2016, 7:12.
33. Xu D, Chen X, He Q, Luo C: MicroRNA-9 suppresses the growth, migration, and invasion of malignant melanoma cells via targeting NRP1. *Onco Targets Ther* 2016, 9:7047-7057.
34. Xu X-Z, Li X-A, Luo Y, Liu J-F, Wu H-W, Huang G: MiR-9 promotes synovial sarcoma cell migration and invasion by directly targeting CDH1. *The International Journal of Biochemistry & Cell Biology* 2019, 112:61-71.
35. Wang WX, Yu HL, Liu X: MiR-9-5p suppresses cell metastasis and epithelial-mesenchymal transition through targeting FOXP2 and predicts prognosis of colorectal carcinoma. *Eur Rev Med Pharmacol Sci* 2019, 23(15):6467-6477.

Figures

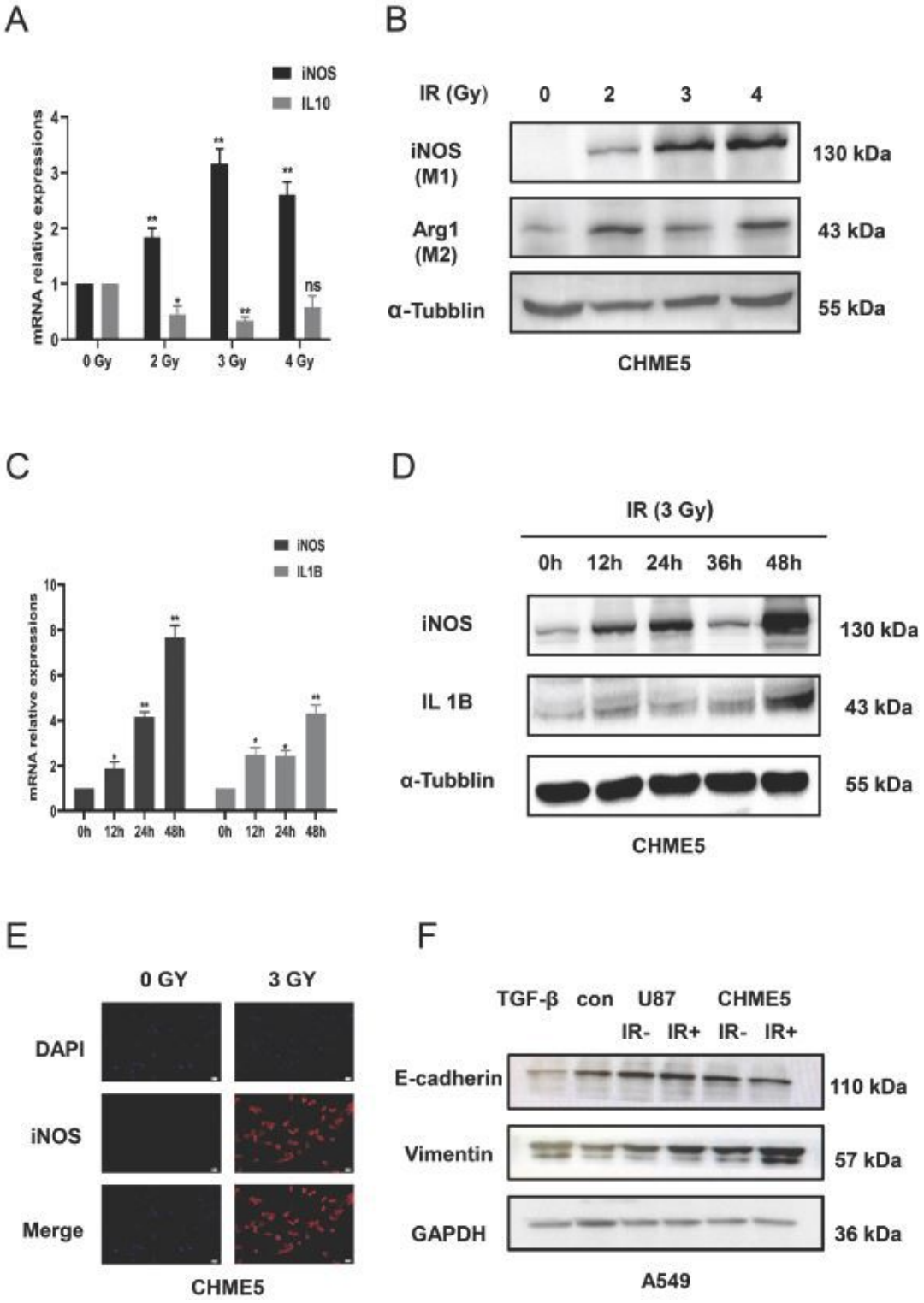

Figure 1

Irradiated microglia exhibited M1 type polarization and hampered A549 cells MET transition (A) qRT-PCR results of iNOS and IL 10 mRNA expression in CHME5 cells after 0, 2, 3, 4 Gy irradiation. (B) Protein expression of Arg1 and iNOS in CHME5 cells after 0, 2, 3, 4 Gy irradiation, α-Tubblin was used as positive control. (C) qRT-PCR results of iNOS and IL 1B mRNA expression in CHME5 cells at different time points (0h; 12h; 24h; 48h) after 3 Gy irradiation. (D) Protein expression of IL1B and iNOS in CHME5 cells at

different time points (0h; 12h; 24h; 36h; 48h) after 3 Gy irradiation. α-Tubblin was used as positive control. (E) Immunofluorescence staining analysis was employed to detect the iNOS (red) in CHME5 cells with or without irradiation (3 Gy for 48h). The blue signal represents the DAPI-stained nuclei. Magnification was 200×. (F) Protein expression of E-cadherin and Vimentin in A549 cells. All groups of A549 cells were firstly treated with TGF-β1(2.5μg/ml). Then controlled culture media, cell culture supernatant of U87 with or without irradiation(IR+/IR-), cell culture supernatant of CHME5 with or without irradiation(IR+/IR-), were added into those TGF-β1 treated A549 cells respectively. IR: irradiation. Data are mean ± SD. ns, $P>0.05$, *$P<0.05$, **$P<0.01$.

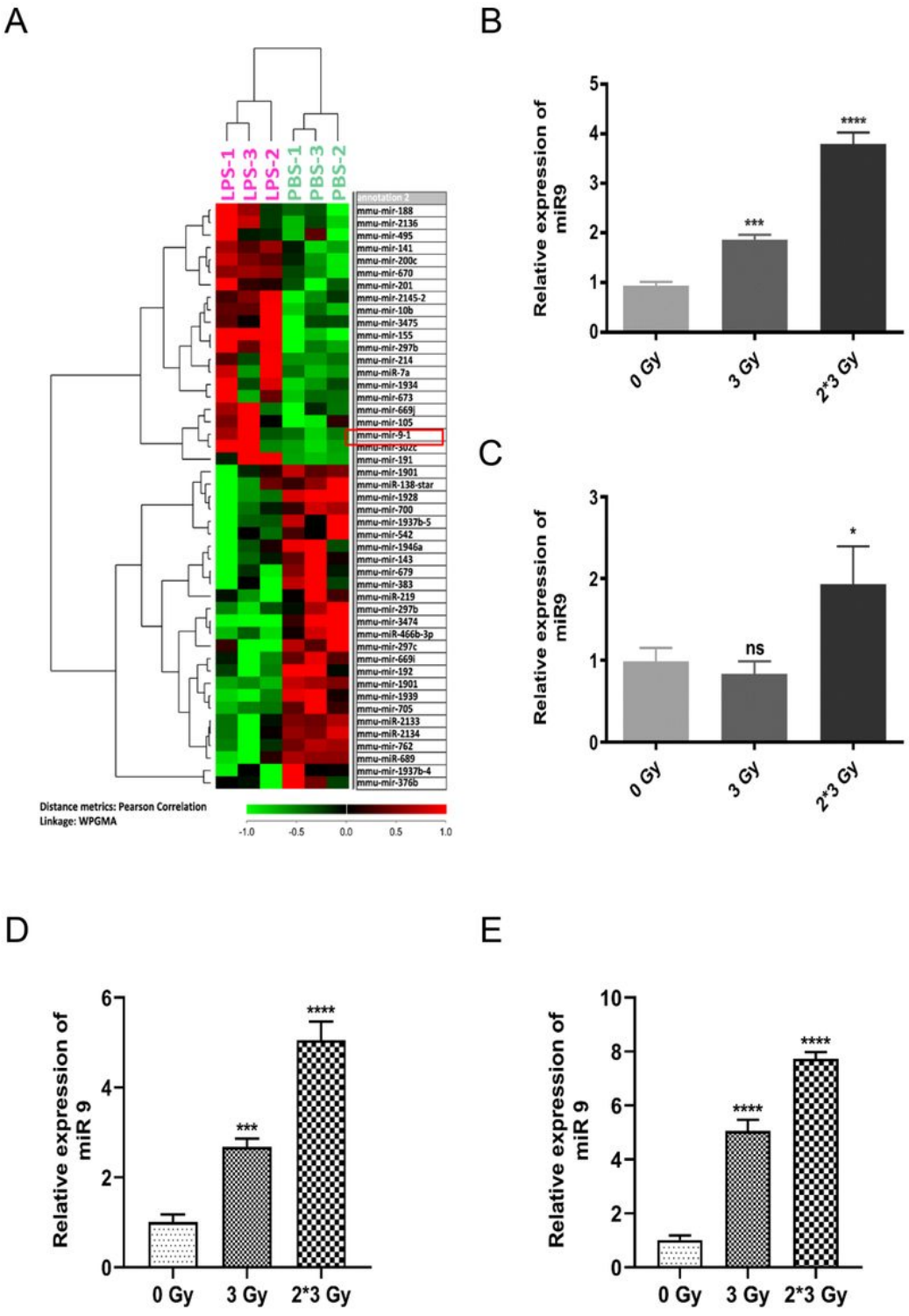

Figure 2

Irradiation-induced M1 type microglia increased both intra and extra-cellular miR-9 level (A) Heat map of miRNA microarray data shows differentially expressed miRNA pattern between LPS-treated and PBS-treated microglia. Red indicates relatively up-regulated genes. Green indicates relatively down-regulated genes. (B) qRT-PCR results of intracellular miR-9 expression in CHME5 cells after 0 Gy, 3 Gy, 3 Gy*2f, irradiation. (C) qRT-PCR results of extracellular miR-9 expression in CHME5 cells after 0 Gy, 3 Gy, 3 Gy*2f,

irradiation. (D) qRT-PCR results of intracellular miR-9 expression in HMO6 cells after 0 Gy, 3 Gy, 3 Gy*2f, irradiation. (E) qRT-PCR results of extracellular miR-9 expression in HMO6 cells after 0 Gy, 3 Gy, 3 Gy*2f, irradiation. Data are mean ± SD. ns, P>0.05, *P<0.05, **P<0.01, ***P<0.001; ****P<0.0001.

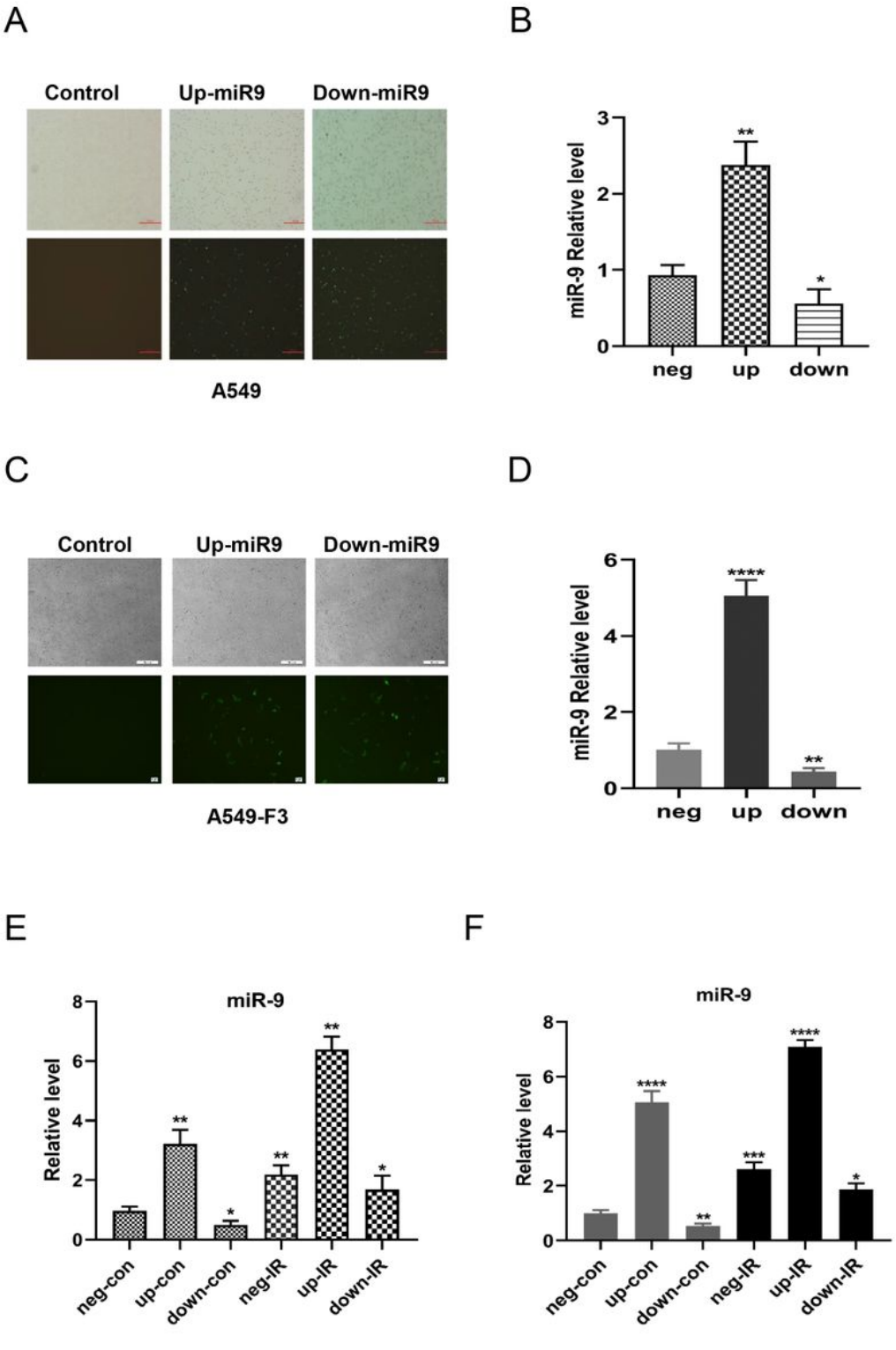

Figure 3

Irradiated M1-type microglia elevated intracellular level of miR-9 in A549 cell lines (A) and (C) Transfection of miR-9 mimic and inhibition plasmid into A549 cells and A549-F3 cells. Magnification was

40×. (B) and (D) qRT-PCR results of intracellular miR-9 expression in A549 cells and A549-F3 cells after transfections of miR-9 mimic and inhibition plasmid. (E) and (F) qRT-PCR results of intracellular miR-9 expression in A549 and A549-F3 cells groups treated with different supernatant. neg-con, negative control plasmid + non-irradiated microglia supernatant; up-con, miR-9 mimic plasmid + non-irradiated microglia supernatant; down-con, inhibition plasmid + non-irradiated microglia supernatant; neg-IR, negative control plasmid + irradiated microglia supernatant; up-IR, miR-9 mimic plasmid + irradiated microglia supernatant; down-IR, inhibition plasmid + irradiated microglia supernatant. Data are mean ± SD. *P<0.05, **P<0.01, ***P<0.001, ****P<0.0001.

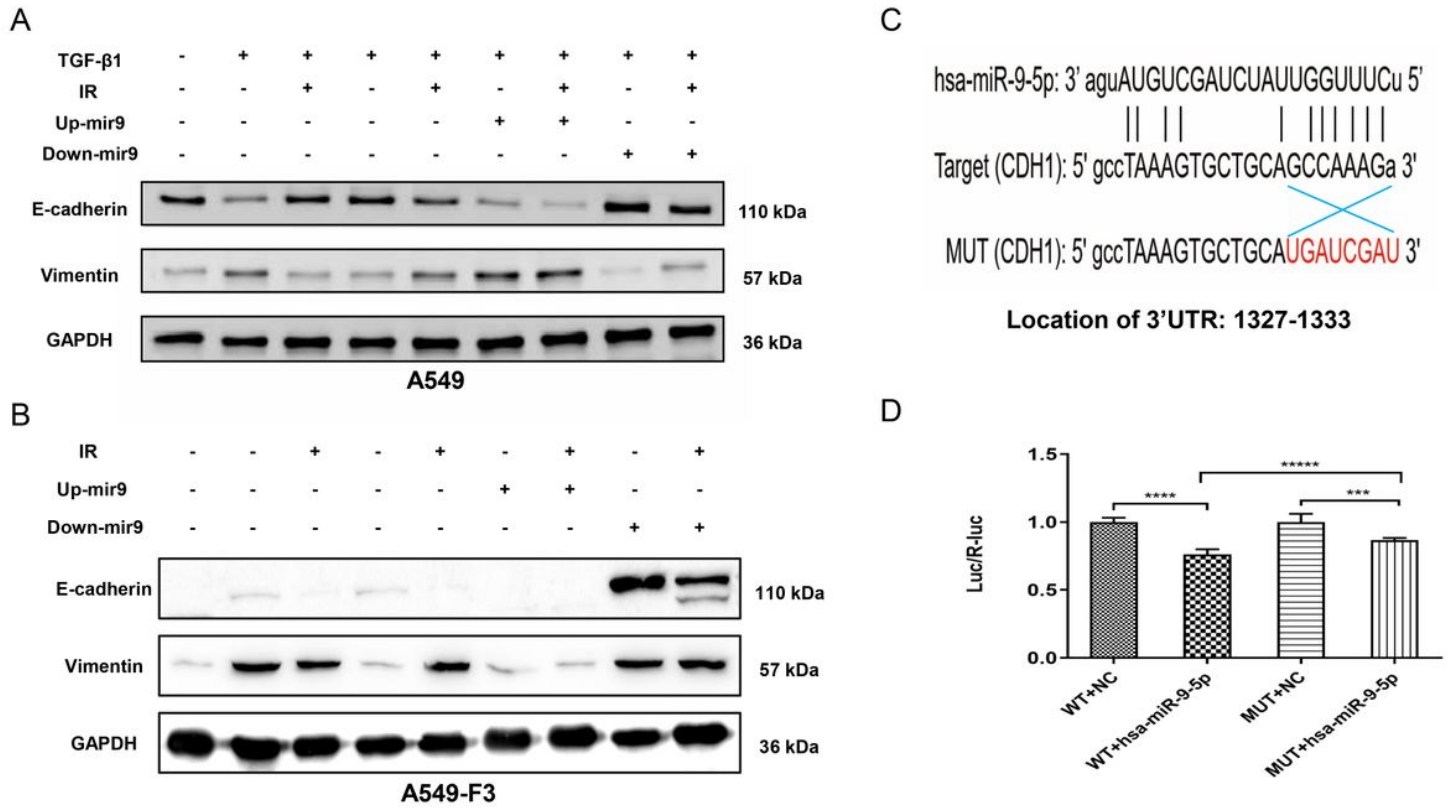

Figure 4

Irradiated M1-microglia increased miR-9 in A549 cell lines and inhibited the MET process (A) and (B) Protein expression of E-cadherin and Vimentin in A549 cells and A549-F3 cells. All groups of A549 cells transfected with negative control, miR-9 mimics (up+), miR-9 inhibition (down+) plasmid were firstly treated with TGF-β1 (TGF-β1+). Then controlled culture media, cell culture supernatant of CHME5 cells with or without irradiation (IR+/IR-), were added into those TGF-β1 treated A549 cells or A549-F3 cells respectively. (C) Schematic representation of the 3'-UTR of CDH1 with the predicted target site for miR-9-5p. The mutant site of CDH1 3'-UTR is indicated as red font (without line). (D) Relative luciferase activity was assayed in different groups. H15279: WT; H15280: MUT; NC: scramble miRNA mimic; miR-9: miR-9-5p mimic. Data are mean ± SD. *P<0.05, **P<0.01, ***P<0.001, ****P<0.0001.

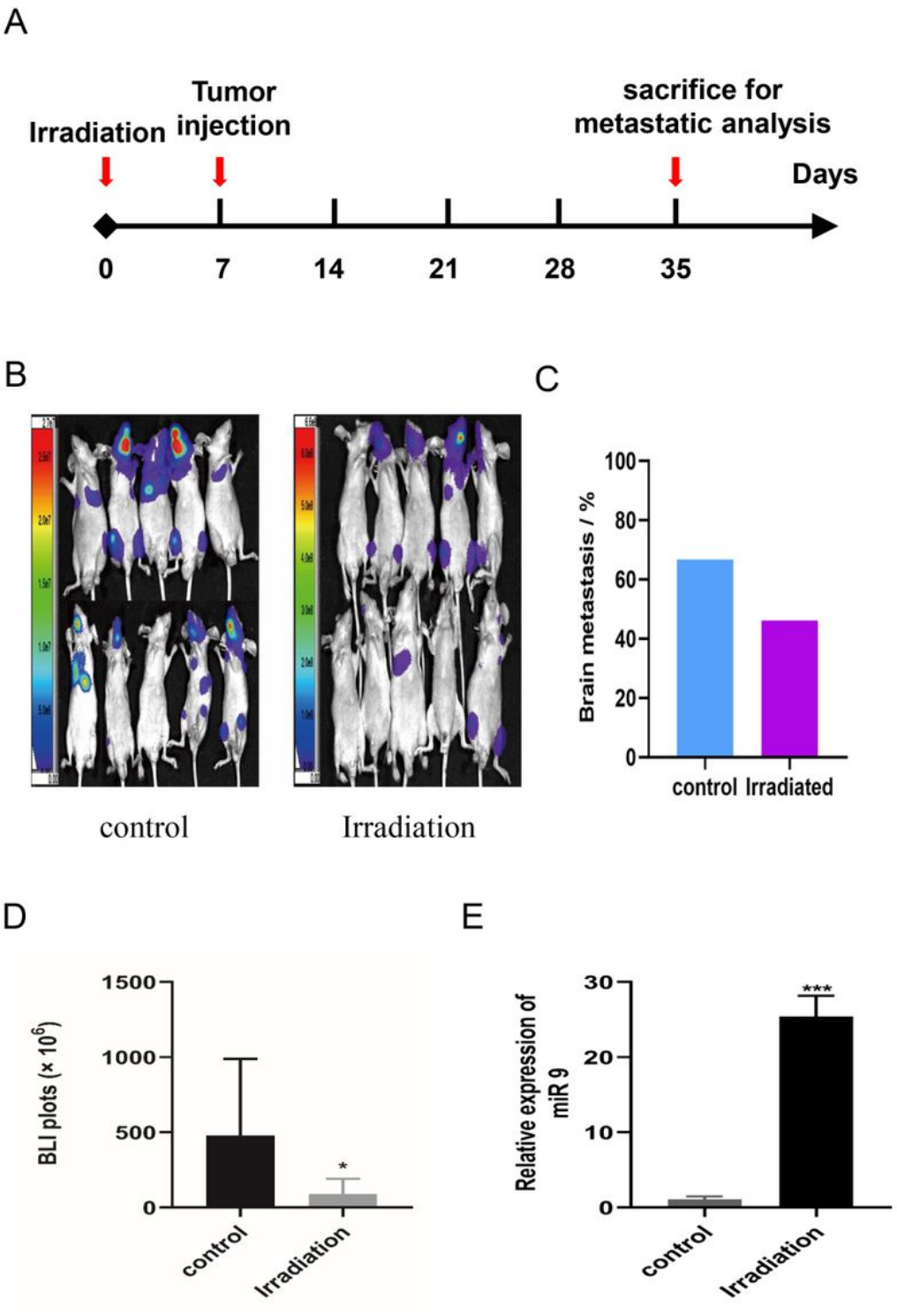

Figure 5

Low dose irradiation reduced brain metastases of A549-F3 cells in brain mice model (A) Schematic diagram illustrates the treatment schedule of irradiation. (B)Brain metastases were determined by bioluminescence imaging in control and irradiated group. (C) Histogram showed incidence of brain metastasis in control and irradiated group. (D) Photon flux detected from brain metastatic focus in

control and irradiated group. (E) qRT-PCR results of miR-9 from brain tissue of mouse treated with or without irradiation. Data are mean ± SD. *P<0.05, **P<0.01, ***P<0.001.

Supplementary Files

This is a list of supplementary files associated with this preprint. Click to download.

- FigureS1.pdf
- TableS1.docx